

## PAPER

# Comparison between T2 Turbo Inversion Recovery Magnitude and T2 Frequency Selective Fat Saturation Turbo Spin Echo MRI Sequences in Detection of Perianal Fistula

Noor Fadhil Baqir<sup>1</sup>(✉),  
Rasha Sabeeh Ahmed<sup>1</sup>,  
Khaleel Ibraheem Mohson<sup>2</sup>

<sup>1</sup>Department of Physiology and Medical Physics, College of Medicine, Al-Nahrain University, Kadhimiya, Baghdad, Iraq

<sup>2</sup>National Cancer Research Center, University of Baghdad, Baghdad, Iraq

[lavendrtechnologist2017@gmail.com](mailto:lavendrtechnologist2017@gmail.com)

## ABSTRACT

Fat suppression magnetic resonance imaging (MRI) sequences are routinely included in the MRI protocol for patients with perianal fistula to improve the visibility of the abnormal tracts and abscesses against the background of hypo-signal intensity on the image. The objective of this study is to compare the turbo inversion recovery magnitude (TIRM) and frequency selective fat saturation turbo spin echo (FSTSE) MRI sequences in detecting perianal fistulas in terms of time and clarity. The MRI protocol included a coronal T2 turbo inversion recovery magnitude sequence, a T2 fat saturation turbo spin echo, and T2 turbo inversion recovery magnitude sequences in the axial plane. The evaluation of sequence image quality involved calculating the signal-to-noise ratio (SNR) and contrast-to-noise ratio (CNR). Additionally three radiologists assessed the best image using a questionnaire designed to align with the study's objectives. The T2 TIRM sequence was found to have the highest number of ticked images. The inter-rater kappa agreement showed fair agreement ( $k = 0.370$ ) between the raters. However, the SNR and CNR values for the T2 FSTSE were higher than those of the T2 TIRM sequence, with a p-value less than 0.001. There is a significant difference in the meantime in that the T2 TIRM sequence has less time than the T2 FSTSE with a p-value  $< 0.001$ . Due to its uniform fat suppression in the MR image and shorter acquisition time, the turbo inversion recovery magnitude sequence exhibited superior performance compared to the T2 frequency-selective turbo spin echo sequence.

## KEYWORDS

perianal fistulas, magnetic resonance imaging (MRI), turbo inversion recovery magnitude (TIRM), frequency selective turbo spin echo (FSTSE)

Baqir, N.F., Ahmed, R.S., Mohson, K.I. (2023). Comparison between T2 Turbo Inversion Recovery Magnitude and T2 Frequency Selective Fat Saturation Turbo Spin Echo MRI Sequences in Detection of Perianal Fistula. *International Journal of Online and Biomedical Engineering (iJOE)*, 19(14), pp. 98–106. <https://doi.org/10.3991/ijoe.v19i14.42557>

Article submitted 2023-06-13. Revision uploaded 2023-07-19. Final acceptance 2023-07-19.

© 2023 by the authors of this article. Published under CC-BY.

## 1 INTRODUCTION

A perianal fistula is an inflammatory condition that causes considerable dilemma in the area around the anal canal [1]. The incidence rate is around two times higher in males than females [2]. Clinically significant symptoms of perianal fistulas include discomfort at the site of the fistula, inflammation, purulent discharge, incontinence, and a low quality of life for the patient [3]. Magnetic resonance imaging (MRI) has superseded alternative imaging methods for perianal fistulas due to its ability to provide the most precise information regarding the anatomy of the fistula tract and its connection to the anal sphincter muscles. By providing these details, MRI increases surgical success rates and decreases rates of perianal fistula recurrence [4] [5]. T2-weighted images with a higher signal from fat can mask diseases with a prolonged T2 in or near the fatty tissue. Two common pre-pulse fat-suppression methods have been employed to address this issue: the turbo inversion recovery magnitude (TIRM) sequence, which is equivalent to short tau inversion recovery (STIR), also called turbo STIR, and the frequency-selective fat saturation turbo spin echo (FSTSE) [6] [7]. TIRM is a sequence that uses the inversion recovery pulse sequence, with the inversion time adjusted to the fat null point. The effectiveness of this sequence relies on the relatively shorter T1 of adipose tissue compared to that of most other tissues. The first 180-degree pulse, known as the “inversion pulse,” inverts all equilibrium magnetizations. The magnetization returns to its initial value,  $M_0$ , as T1 recovers. Fat-based tissues do not generate any signal when the 90-degree pulse is applied at the null point of fatty tissue because there is no shifting into the x-y plane upon applying the pulse [8] [9]. TIRM sequences are often performed with fast spin echo sequences [10] [11]. FSTSE relies on the observation that the resonance frequencies of water and fat differ by 3.5 ppm (parts per million). Therefore, utilizing a narrow spectrum of RF frequencies centered on the fat Larmor frequency, protons in fat are given a 90° pulse while water protons remain unexcited. This pulse type is a chemical shift selective (CHESS) pulse. The imaging sequence is initiated immediately after the CHESS pulse, preventing fat from recovering its longitudinal magnetization, resulting in an image with a reduced fat signal [9] [12] [13]. Therefore, is there any difference between TIRM and frequency-selective FSTSE MRI sequences regarding the clarification of perianal fistulas and acquisition time.

Nakatsu et al. [14] aimed to compare the uniformity of fat suppression and lesion conspicuity between short inversion time inversion recovery (STIR) fast spin-echo (FSE), which is equivalent to TIRM and fat-saturated T2-weighted FSE sequences for magnetic resonance (MR) imaging of the neck and thorax. The prospective study comprised a sample of 40 consecutive patients. MR imaging used a 1.5 Tesla system. The homogeneity of fat suppression (with n equal to 40) and the conspicuousness of lesions (with n equal to 35) were evaluated. In STIR, FSE and fat-saturated T2-weighted FSE images were evaluated by three radiologists using quantitative analyses (a five-point rank score). The reference images used for comparison were FSE without fat saturation. The STIR FSE sequence demonstrated success in all patients. The statistical analysis revealed that the STIR and fat-saturated FSE techniques had mean scores of 4.3 and 2.3, respectively, in terms of homogeneity of fat suppression. This difference was statistically significant, with a p-value of less than 0.0001. The statistical analysis found that the mean scores for lesion conspicuity were 4.3 and 3.5 for the STIR and fat-saturated FSE techniques, respectively ( $p < 0.0001$ ). Consequently, the STIR FSE technique proves

to be a reliable clinical approach that produces magnetic resonance images with consistent fat suppression.

The purpose of this study is to make a comparison between the TIRM and FSTSE MRI sequences in the detection of perianal fistulas (the best one for the radiologist) regarding time and perianal fistula clarification.

## 2 MATERIALS AND METHODS

### 2.1 Data collection

From December 2022 to May 2023, a cross-sectional, non-randomized study was conducted in the MRI department of the oncology teaching hospital in Medical City, Baghdad, Iraq. Based on a physical examination, the surgical outpatient clinics referred fifty patients who were suspected of having perianal fistulas. All participants provided informed written consent, and the study was approved by the institution's ethics committee.

**Inclusion criteria:** This study includes adult individuals of both genders who have a perianal fistula, as determined through a physical examination, and who were referred from outpatient surgical clinics. **Exclusion criteria** include children, pregnant women, and any patients contraindicated for MRI examination, such as those with cardiac pacemakers or metallic implants, as well as patients with claustrophobia.

Magnetic resonance imaging exams were conducted utilizing 1.5 T (Magnetom Aera, Siemens Healthcare, Germany) scanners equipped with a phased-array surface coil consisting of 18 channels. No patient preparation was necessary prior to the examination. On the MRI table, patients lay flat on their backs, and a phased array surface coil was put on their pelvic area. Maintaining proper orientation when using MR to image the anal canal is important. The images' planning is accomplished using a sagittal T2-weighted localizer that passes through the patient's midline. The oblique transverse and coronal sections are aligned orthogonally and parallel to the anal sphincter, respectively. The MRI sequence parameters used in this study were as follows: T2 TIRM in the oblique coronal plane (TR/TE: 5000/50, flip angle: 140°, slice thickness: 3 mm, interstice gap: 20%, FOV: 390 mm, number of slices: 34, matrix size: 384 × 288, inversion time (TI): 160 s, signal averages: 1, acquisition time: 2:27 (min: sec)). T2 TIRM in the oblique axial plane (TR/TE: 5040/50 ms, flip angle: 149°, slice thickness: 3 mm, interstice gap: 20%, FOV: 380 mm, number of slices: 36, matrix size: 384 × 234, inversion time (TI): 160 s, signal averages: 1, acquisition time: 2:02 (min: sec)), the T2 FS TSE in the oblique axial plane (TR/TE: 5170/65, flip angle: 150°, slice thickness: 3 mm, interstice gap: 30%, FOV: 380 mm, matrix size: 448 × 284, number of slices: 36, signal averages 1: acquisition time: 2:07 (min: sec)), and T1 FS TSE in oblique axial plane pre and post administration of contrast media (TR/TE: 619/20, flip angle: 160°, slice thickness: 3 mm, interstice gap: 20%, FOV: 239 mm, matrix size: 192 × 163, number of slices: 27, signal averages 1: acquisition time: 1:55 (min: sec)).

### 2.2 Qualitative assessment of image

For the assessment of the two images, TIRM and FSTSE, four radiologists with a high degree in radio diagnosis, more than five years of experience in MRI reporting, and more than 40 reports per week were selectively chosen to be employed in the oncology teaching hospital as they got higher ranks among their colleagues. Those

radiologists reviewed the two imaging data sets with a questionnaire (yes or no) that included the following parameters:

- T2 TIRM axial
- T2 FS TSE axial
- If both of them select the best one, please.

### 2.3 Quantitative assessment of image

Under the supervision of the radiologist, the assessment of MR image quality involves the calculation of signal-to-noise ratio (SNR) and contrast-to-noise ratio (CNR) using two regions of interest (ROI): one in the fistula site and the other in the nearest normal tissue. The calculation of the SNR and CNR was performed with (the Radiant DICOM viewer 2022.1.1) program. The SNR was calculated with the equation [10]:

$$SNR = \frac{\text{signal pathological}}{\text{standard deviation of noise}} \quad (1)$$

CNR was calculated using the equation [11]:

$$CNR = \frac{\text{signal pathological} - \text{signal normal tissue}}{\text{standard deviation of noise}} \quad (2)$$

The pathological signal is obtained when the ROI is placed on the area of the perianal fistula. A normal tissue signal is obtained when the ROI is placed on the area of normal tissue near the fistula. The mean of the areas of ROI obtained was (0.32 mm<sup>2</sup>). The noise background standard deviation is taken as an average of the four corner regions in the image.

### 2.4 Statistical analysis

The data were fed to the system, coded, and examined using the statistical package for social sciences (SPSS) version 26.

The data were presented by frequencies and percentages if qualitative and by means  $\pm$  standard deviations if quantitative. Shapiro Wilk and Kolmogorov-Smirnov tests assessed whether quantitative data were normally distributed. A paired sample t-test, or Wilcoxon signed rank test, was used to evaluate differences between two related continuous variables. The Mann-Whitney U test was employed to evaluate the distinction between two independent samples. A P-value equal to or less than 0.05 was considered significant. This study used the Fleiss Kappa test for reliability to assess the inter-rater agreement of more than two raters.

## 3 EXPERIMENTAL PROCEDURE

The study results were obtained from 50 patients clinically diagnosed with perianal fistula. Most (82%) of those patients with anal fistula were males, while the remaining 18% were females. The average age of all patients under test was  $39 \pm 12.46$  years.

Table 1 shows a significant difference between T2 TIRM and T2 FS TSE in SNR value with a P-value less than 0.001. The T2 FS TSE had a higher mean ( $82.12 \pm 29.93$ ) when compared to T2 TIRM ( $53.12 \pm 14.00$ ). Regarding CNR, there is also a significant (P-value < 0.001) difference between the two sequences. The mean  $\pm$  SD for T2 FS TSE was ( $50.28 \pm 28.60$ ), while for T2 TIRM, it was ( $31.10 \pm 11.39$ ).

**Table 1.** Mean SNR, CNR of the T2 TIRM, FS TSE

| Sequences | Mean SNR          | Mean CNR          |
|-----------|-------------------|-------------------|
| T2 TIRM   | $53.12 \pm 14.00$ | $31.10 \pm 11.39$ |
| T2 FS TSE | $82.12 \pm 29.93$ | $50.28 \pm 28.60$ |
| P-value   | < 0.001           | < 0.001           |

Table 2 shows the frequency distribution of the raters' answers about the visualization of fistulas by different MRI sequences according to the prepared questionnaire. It found that the three raters ticked most of the images for the T2 TIRM sequence. Rater number 2 mentioned that 48 out of 50 (96%) images demonstrated the presence of fistula in T2 TIRM, followed by 92% by Rater 3 and 84% by Rater number 1. About T2 FS TSE, rater 2 mentioned that they could visualize an anal fistula in only two images out of 50 (4%). The highest percentage was demonstrated by rater one, who found the fistula in eight (16%) images.

The inter-rater kappa agreement was performed to test the reliability of the questionnaire used to evaluate MRI images obtained for the visualization of 50 patients clinically diagnosed with perianal fistula, as shown in Table 3. The test statistic result indicates a significant (P-value < 0.001) and moderate ( $k = 0.370$ ) agreement among the three raters regarding the use of T2 TIRM versus T2FS TSE for the specific question, as demonstrated in Figure 1. Comparing the time required for the two MRI sequences used in this study is established in Table 4. Even a small difference was demonstrated in T2 TIRM and T2 FS TSE. The observed difference was statistically significant (P-value < 0.001).

**Table 2.** Frequency and percentage of T2 TIRM, T2 FS TSE for three raters

|         | Frequency (Percentage) T2 TIRM | Frequency (Percentage) T2 FS TSE |
|---------|--------------------------------|----------------------------------|
| Rater 1 | 42 (84%)                       | 8 (16%)                          |
| Rater 2 | 48 (96%)                       | 2 (4%)                           |
| Rater 3 | 46 (92%)                       | 4 (8%)                           |

**Table 3.** Inter-rater reliability and overall agreement between physicians in the diagnosis of perianal fistula among 50 patients

| Sequences            | Kappa | 95% Confidence Interval (CI) | P-Value |
|----------------------|-------|------------------------------|---------|
| T2 TIRM vs T2 FS TSW | 0.370 | 0.365 – 0.375                | < 0.001 |

**Table 4.** Time difference between T2 TIRM and T2 FS TSE

| Sequence  | Mean $\pm$ Standard Deviation (SD) | P-Value |
|-----------|------------------------------------|---------|
| T2 TIRM   | $2:02 \pm 0.02$                    | < 0.001 |
| T2 FS TSE | $2:08 \pm 0.02$                    |         |

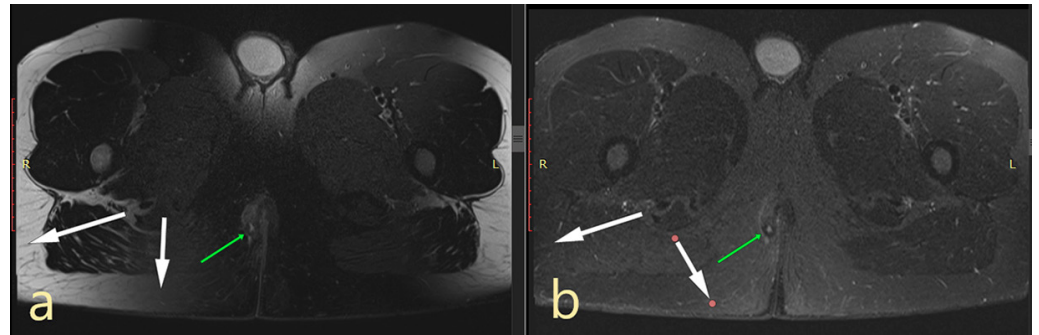


**Fig. 1.** A female patient, aged 40, who presented with perianal fistula (green arrow); a: T2 FS TSE in the oblique axial plane shows uneven fat suppression (white arrow); and b: T2 TIRM in the oblique axial plane shows even fat suppression (white arrow)

#### 4 DISCUSSIONS

In patients with suspected perianal inflammatory diseases (e.g., fistulous disease), fat-suppressed T2-weighted sequences (either TIRM or frequency-selective fat-saturation) are added to the protocol. This addition enhances the visibility of fluid-containing tracts and abscesses, thereby facilitating the detection of small tracts [15]. No studies have compared T2 TIRM and FSTSE in terms of their ability to detect perianal fistulas in relation to time, SNR, or CNR. In our research, the SNR and CNR showed significant differences between the T2 FS TSE and T2 TIRM sequences (p-value was less than 0.001). This finding is consistent with Bloem et al. [16], who attributed the higher SNR in T2 FS TSE more than the inversion recovery sequence (TIRM).

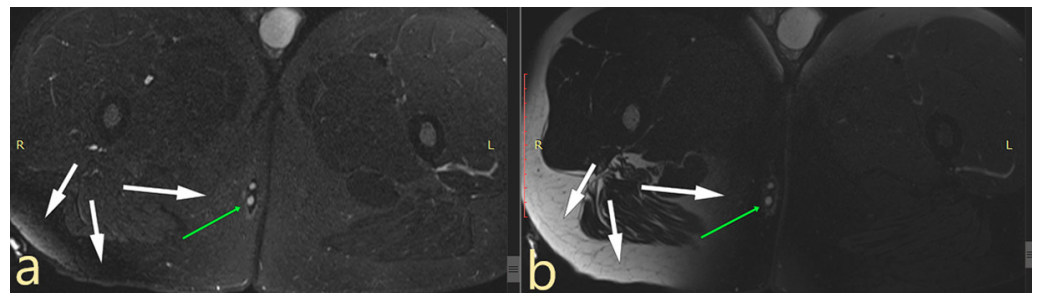


**Fig. 2.** A male, 20-year-old, presenting with perianal fistula (green arrow); a: T2 TIRM image in the oblique axial plane representing even fat suppression (white arrow); b: T2 FS TSE image in the oblique axial plane showing uneven fat suppression (white arrow)

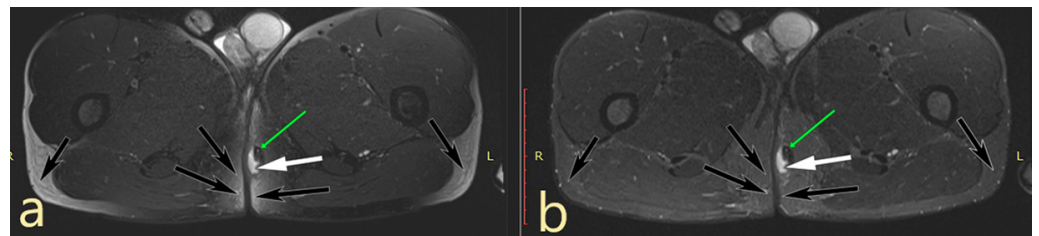


**Fig. 3.** A male, 32-year-old, presenting with perianal fistula (small green arrow) and inflammatory changes (white arrow); a: T2 FS TSE image in the oblique axial plane demonstrating uneven fat suppression (black arrow), and b: T2 TIRM image in the oblique axial plane demonstrating even fat suppression in the site of the fistula and edge of the image (thick black arrow)

The principle behind fat suppression in the FS TSE sequence lies in the distinct resonance frequency difference of approximately 3.5 ppm between fat and water. Consequently, during the acquisition of T2 FSTSE, a resonance frequency pulse is applied that aligns with the resonance frequency of white fat.

White fat comprises lobules that are separated by loose connective tissue septa and supported by stroma. During the MRI acquisition, two distinct components contribute to the signal from white fat. Lipids primarily generate the signal, accounting for more than 80% of it.

In comparison, protons from hydrogen atoms in the water within the loose connective tissue contribute to less than 20% of the signal. T2 FS TSE is a lipid-specific sequence with high SNR and CNR. However the inhomogeneity of the static magnetic field may alter the resonance frequency of water and fat. In these specific areas, the resonance frequency of the saturation (CHES) pulse could not be aligned with the resonance frequency of lipids, leading to insufficient fat suppression [17]. Areas characterized by fluid, pus, and granulation tissue exhibit high signal intensity against a low background in imaging [1]. However, the qualitative assessment in our study showed that the TIRM sequence was preferable compared to the FS TSE in the detection of perianal fistula among 50 patients ( $\kappa = 0.370$ ), which means a fair agreement between them, as illustrated in Figures 2 and 3. The average rater's sensitivity for TIRM replacing FS TSE was (90.7%), taking the physical examination as the gold standard. That agreed with Jabeen et al. [18], who showed the diagnostic accuracy of STIR (equivalent to TIRM) as a limited protocol in diagnosing perianal fistula in a developing country, with the sensitivity of STIR at 96.6% taking the surgical reports as a gold standard.

The advantage of TIRM over FS TSE is the uniformity of the fat suppression produced by the TIRM pulse sequence due to the basic principles of nulling the white fat signal and the tissue signals with a short T1 similar to fat [17], and the strong insensitivity to  $B_0$  inhomogeneity in contrast to FS TSE [19], means the TIRM sequence can be relied on even in challenging anatomical locations, such as perianal fistula, which shows up as a strip or band of tissue with high signal intensity, clearly distinguishable from the surrounding muscle and fat [20]. Nakatsu et al. [14] reported that the STIR FSE (equivalent to TIRM) is reported as superior to the T2 FS TSE in cervical and thoracic magnetic resonance imaging regarding the lesion conspicuity and homogeneity of fat suppression. In addition, our study demonstrated a significant difference statistically for the acquisition time of the T2 TIRM sequence, which was less than the T2 FS TSE with a p-value less than 0.001, making it preferable.

In postoperative patients, the presence of a foreign body can cause modifications in the local magnetic field, leading to the generation of a susceptibility artifact. Susceptibility refers to the ability of a material to cause distortion or alteration in a static magnetic field. The artifact is typically observed at the boundary or interface between substances with different magnetic susceptibilities. MR imaging artifacts in postoperative patients can be attributed to suture artifacts, such as a seton implanted along the fistula track. Among various types of sutures, silk is commonly utilized and known to induce the most prominent susceptibility artifact compared to other suture materials. However, the TIRM sequence is an effective alternative strategy that relies less on the homogeneity of the primary magnetic field to achieve signal suppression. TIRM imaging reduces susceptibility effects in fat-suppressed imaging by utilizing T1 relaxation differences instead of precessional frequency differences (as seen in FS TSE sequences) to nullify the signal originating from fat [1].

There are several limitations to our study. First, the small sample size, and second, the study was conducted at a single center. Therefore, it is recommended to conduct multi-centric studies with a larger sample size in our population.

## 5 CONCLUSION

Our study showed the preferable T2 fat suppression sequence for detecting perianal fistulas. The TIRM technique demonstrated superiority over the T2 frequency-selective fat saturation sequence. Despite the lowering of SNR and CNR of the TIRM sequence, TIRM provides uniform fat suppression even at the edge of the image and is less affected by  $B_0$  inhomogeneity and susceptibility artifacts caused by a foreign body in postoperative patients, with less adequate time of two minutes and two seconds.

## 6 ACKNOWLEDGMENT

The authors thank the reviewers for their comments and suggestions for improving the paper.

## 7 REFERENCES

- [1] J. de Miguel Criado *et al.*, “MR imaging evaluation of perianal fistulas: Spectrum of imaging features,” *Radiographics*, vol. 32, no. 1, pp. 175–194, 2012. <https://doi.org/10.1148/rg.321115040>
- [2] G. Gurung, “3T MR imaging evaluation of perianal fistulas: An initial experience in Nepal,” *Journal of Society of Surgeons of Nepal*, vol. 19, no. 1, pp. 25–30, 2016. <https://doi.org/10.3126/jssn.v19i1.24552>
- [3] M. Włodarczyk, J. Włodarczyk, A. Sobolewska-Włodarczyk, R. Trzciński, Ł. Dziki, and J. Fichna, “Current concepts in the pathogenesis of cryptoglandular perianal fistula,” *Journal of International Medical Research*, vol. 49, no. 2, 2021. <https://doi.org/10.1177/0300060520986669>
- [4] N. Akyel, K. Akin, D. Kösehan, and A. Köktener, “Perianal fistula imaging: A comparison between two-channel superficial Flex coil and eight-channel body coil,” *Polish Journal of Radiology*, vol. 84, pp. 430–435, 2019. <https://doi.org/10.5114/pjr.2019.89906>
- [5] J. Y. R. Al-Awadi, H. K. Aljobouri, and A. M. Hasan, “MRI brain scans classification using extreme learning machine on LBP and GLCM,” *International Journal of Online & Biomedical Engineering*, vol. 19, no. 2, 2023. <https://doi.org/10.3991/ijoe.v19i02.33987>
- [6] M. Sadick, H. Sadick, K. Hörmann, C. Düber, and S. J. Diehl, “Diagnostic evaluation of magnetic resonance imaging with turbo inversion recovery sequence in head and neck tumors,” *European Archives of Oto-Rhino-Laryngology and Head & Neck*, vol. 262, pp. 634–639, 2005. <https://doi.org/10.1007/s00405-004-0878-x>
- [7] K. Tanabe, K. Nishikawa, T. Sano, O. Sakai, and H. N. Jara, “Fat suppression with short inversion time inversion-recovery and chemical-shift selective saturation: A dual STIR-CHESS combination prepulse for turbo spin echo pulse sequences,” vol. 31, no. 5, pp. 1277–1281, 2010. <https://doi.org/10.1002/jmri.22147>
- [8] H. K. Omer, H. A. Jalab, A. M. Hasan, and N. E. Tawfiq, “Combination of local binary pattern and face geometric features for gender classification from face images,” in *9th IEEE International Conference on Control System, Computing and Engineering (ICCSCE)*, IEEE, 2019, pp. 158–161. <https://doi.org/10.1109/ICCSCE47578.2019.9068593>
- [9] D. W. McRobbie, E. A. Moore, M. J. Graves, and M. R. Prince, “MRI from picture to proton,” Cambridge university press, 2017. <https://doi.org/10.1017/9781107706958>
- [10] V. M. Runge, W. R. Nitz, S. H. Schmeets, W. H. Faulkner, and N. K. Desai, “The physics of clinical MR taught through images,” Springer, 2009. <https://doi.org/10.1055/b-002-59228>

- [11] J. Y. Rbat, H. K. Aljobouri, and A. M. Hasan, "MRI brain tumor classification using robust Convolutional Neural Network CNN approach," in *Iraqi International Conference on Communication and Information Technologies (IICCIT)*, IEEE, 2022, pp. 258–261.
- [12] P. Sprawls, "Magnetic resonance imaging: Principles, methods, and techniques," Medical Physics Publishing Madison, 2000.
- [13] A. M. Hasan, H. A. Jalab, F. Meziane, H. Kahtan, and A. S. Al-Ahmad, "Combining deep and handcrafted image features for MRI brain scan classification," *IEEE Access*, vol. 7, pp. 79959–79967, 2019. <https://doi.org/10.1109/ACCESS.2019.2922691>
- [14] M. Nakatsu *et al.*, "Comparison of short inversion time inversion recovery (STIR) and fat-saturated (chemsat) techniques for background fat intensity suppression in cervical and thoracic MR imaging," *Journal of Magnetic Resonance Imaging: An Official Journal of the International Society for Magnetic Resonance in Medicine*, vol. 11, no. 1, pp. 56–60, 2000. [https://doi.org/10.1002/\(SICI\)1522-2586\(200001\)11:1<56::AID-JMRI8>3.0.CO;2-D](https://doi.org/10.1002/(SICI)1522-2586(200001)11:1<56::AID-JMRI8>3.0.CO;2-D)
- [15] D. B. Erlichman, D. Kanmaniraja, M. Kobi, and V. Chernyak, "MRI anatomy and pathology of the anal canal," *Journal of Magnetic Resonance Imaging*, vol. 50, no. 4, pp. 1018–1032, 2019. <https://doi.org/10.1002/jmri.26776>
- [16] J. Bloem, M. Reijnierse, T. Huizinga, and A. van der Helm-van Mil, "MR signal intensity: Staying on the bright side in MR image interpretation," *RMD Open*, vol. 4, 2018. <https://doi.org/10.1136/rmdopen-2018-000728>
- [17] E. M. Delfaut, J. Beltran, G. Johnson, J. Rousseau, X. Marchandise, and A. Cotten, "Fat suppression in MR imaging: Techniques and pitfalls," *Radiographics*, vol. 19, no. 2, pp. 373–382, 1999. <https://doi.org/10.1148/radiographics.19.2.g99mr03373>
- [18] N. Jabeen, R. Qureshi, A. Sattar, and M. Baloch, "Diagnostic accuracy of short tau inversion recovery as a limited protocol for diagnosing perianal fistula," (in eng), *Cureus*, vol. 11, no. 12, 2019. <https://doi.org/10.7759/cureus.6398>
- [19] T. A. Bley, O. Wieben, C. J. François, J. H. Brittain, and S. B. Reeder, "Fat and water magnetic resonance imaging," *Journal of Magnetic Resonance Imaging*, vol. 31, no. 1, pp. 4–18, 2010. <https://doi.org/10.1002/jmri.21895>
- [20] G. Lo Re *et al.*, "MR imaging of perianal fistulas in Crohn's disease: Sensitivity and specificity of STIR sequences," *La Radiologia Medica*, vol. 121, pp. 243–251, 2016. <https://doi.org/10.1007/s11547-015-0603-4>

## 8 AUTHORS

**Noor Fadhil Baqir** received B.Sc. degree in radiological techniques from Middle Technical University, College of Medical and Health Techniques. She is working as MRI technologist at oncology teaching hospital in Medical City, Baghdad, Iraq.

**Rasha Sabeeh Ahmed** received the B.Sc. degree in physics from Mustansiriyah University, Iraq; M.Sc. degree in atomic physics from Mustansiriyah University, Iraq; and Ph.D. in nuclear physics from Baghdad University. She is currently working as a Professor at Physiology and Medical Physics Department, College of Medicine, Al-Nahrain University, Baghdad, Iraq. She has authored more than 25 indexed papers. Her research interests include nuclear medical physics, atomic physics, nuclear physics, and environmental physics.

**Khaleel Ibraheem Mohson, MD** is an Assistant professor of Radiology-University of Baghdad, Head of Clinical Department–National Cancer Research Center, University of Baghdad, and as Supervisor and trainer in Iraqi and Arabic boards of Radiology.